



ARTICLE

# Cyclin B3 is required for metaphase to anaphase transition in oocyte meiosis I

Yufei Li<sup>1,2\*</sup>, Leyun Wang<sup>1,2\*</sup>, Linlin Zhang<sup>1,3\*</sup> , Zhengquan He<sup>1,2\*</sup>, Guihai Feng<sup>1,2</sup>, Hao Sun<sup>1,3</sup>, Jiaqiang Wang<sup>1,2</sup>, Zhikun Li<sup>1,2</sup>, Chao Liu<sup>1,3</sup>, Jiabao Han<sup>1,3</sup>, Junjie Mao<sup>1,3</sup>, Pengcheng Li<sup>1,4</sup>, Xuwei Yuan<sup>1,4</sup>, Liyuan Jiang<sup>1,4</sup>, Ying Zhang<sup>1,2</sup>, Qi Zhou<sup>1,2,3</sup>, and Wei Li<sup>1,2,3</sup> 

**Meiosis with a single round of DNA replication and two successive rounds of chromosome segregation requires specific cyclins associated with cyclin-dependent kinases (CDKs) to ensure its fidelity. But how cyclins control the distinctive meiosis is still largely unknown. In this study, we explored the role of cyclin B3 in female meiosis by generating *Ccnb3* mutant mice via CRISPR/Cas9. *Ccnb3* mutant oocytes characteristically arrested at metaphase I (MetI) with normal spindle assembly and lacked enough anaphase-promoting complex/cyclosome (APC/C) activity, which is spindle assembly checkpoint (SAC) independent, to initiate anaphase I (AnI). Securin siRNA or CDK1 inhibitor supplements rescued the MetI arrest. Furthermore, CCNB3 directly interacts with CDK1 to exert kinase function. Besides, the MetI arrest oocytes had normal development after intracytoplasmic sperm injection (ICSI) or parthenogenetic activation (PA), along with releasing the sister chromatids, which implies that *Ccnb3* exclusively functioned in meiosis I, rather than meiosis II. Our study sheds light on the specific cell cycle control of cyclins in meiosis.**

## Introduction

The meiotic cell cycle, which comprises two consecutive M phases, is crucial for production of haploid germ cells. In both mitotic and meiotic cell cycles, M phases share cyclin B-CDK1 as the key controller to ensure the reliability of cell cycle progression. During prometaphase (pro-MetI), spindle assembly checkpoint (SAC) proteins sequester Cdc20, the anaphase-promoting complex/cyclosome (APC/C) activator, and prevent it from promoting securin and cyclin B ubiquitylation (Thornton and Toczyski, 2003). In metaphase, when all kinetochores are attached to microtubules, Cdc20 liberates from SAC and leads to complete APC/C activity with degradation of both securin and cyclin B. Securin is an inhibitory chaperone of separase, and its destruction promotes separase cleavage of cohesin complexes, which initiates sister-chromatid separation and anaphase onset (Uhlmann et al., 1999). Meanwhile, the degradation of cyclin B reduces maturation-promoting factor or mitosis-promoting factor (MPF) activity and further improves the activity of separase and Cdh1-induced APC/C activation, which guarantees anaphase progression (Vázquez-Novelle et al., 2014).

Cyclin synthesis and degradation cooperate with cyclin-dependent kinases (CDKs) to control the progression of

meiosis and mitosis. Although most of the basic cyclins used in the meiosis metaphase are analogous to those used in mitosis, the lingering question is whether the proofreading function of cyclins during mitosis are equally significant during meiotic division. The primary cyclins in metaphase are B-type cyclins, which contain at least three types of cyclin B (cyclin B1, B2, and B3) in mammals, and it appears that cyclin B1 (*Ccnb1*) is primarily responsible for MPF activity (Jones, 2004). Mice lacking *Ccnb1* were not viable, whereas cyclin B2-null mice had no apparent defects (Brandeis et al., 1998). However, recent reports showed cyclin B2 could compensate for *Ccnb1* in oocyte meiosis I (Li et al., 2018), which implies that there are specific modulations in the meiotic cell cycle regulation.

Cyclin B3 (*Ccnb3*) shares homology with A- and B-type cyclins (Gallant and Nigg, 1994) and is conserved during higher eukaryote evolution (Sigrist et al., 1995; Jacobs et al., 1998; Parry and O'Farrell, 2001; Lozano et al., 2002; Nguyen et al., 2002; Refik-Rogers et al., 2006; Tarailo-Graovac and Chen, 2012; Zhang et al., 2015). Previous studies have shown that females lacking *Ccnb3* are sterile, with oocytes unable to complete

<sup>1</sup>State Key Laboratory of Stem Cell and Reproductive Biology, Institute of Zoology, Chinese Academy of Sciences, Beijing, China; <sup>2</sup>Institute for Stem Cell and Regeneration, Chinese Academy of Sciences, Beijing, China; <sup>3</sup>University of Chinese Academy of Sciences, Beijing, China; <sup>4</sup>College of Life Science, Northeast Agricultural University of China, Harbin, China.

\*Y. Li, L. Wang, L. Zhang, and Z. He contributed equally to this paper; Correspondence to Wei Li: [liweili@ioz.ac.cn](mailto:liweili@ioz.ac.cn); Qi Zhou: [zhouqi@ioz.ac.cn](mailto:zhouqi@ioz.ac.cn); Ying Zhang: [yingzhang@ioz.ac.cn](mailto:yingzhang@ioz.ac.cn).

© 2019 Li et al. This article is distributed under the terms of an Attribution-Noncommercial-Share Alike-No Mirror Sites license for the first six months after the publication date (see <http://www.rupress.org/terms/>). After six months it is available under a Creative Commons License (Attribution-Noncommercial-Share Alike 4.0 International license, as described at <https://creativecommons.org/licenses/by-nc-sa/4.0/>).

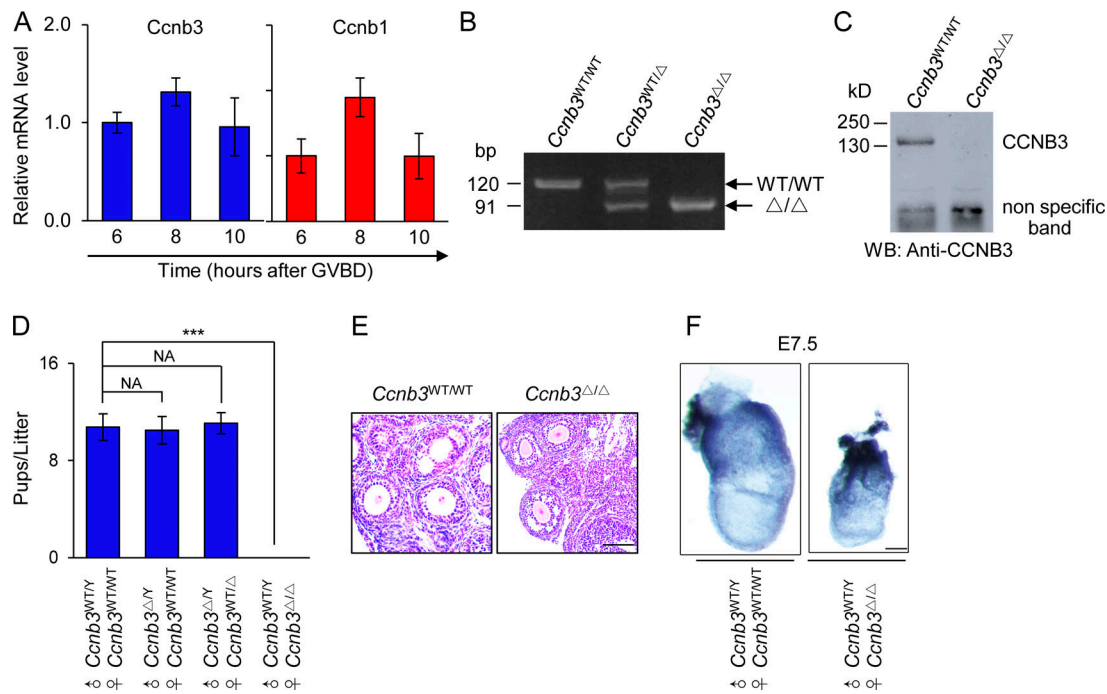


Figure 1. **Ccnb3** mutation led to female infertility in mice. **(A)** The mRNA expression pattern of *Ccnb1* and *Ccnb3* in mouse oocytes during IVM ( $n = 40$  in each group). **(B)** The genotype analysis of *Ccnb3* mutant mice by PCR. **(C)** IP and Western blot analysis of adult testes extracts using anti-CCNB3 antibody, which recognizes an N-terminal epitope. **(D)** Litter size counts showing that *Ccnb3*<sup>Δ/Δ</sup> mice mating with WT male mice failed to produce full-term offspring. At least 20 *Ccnb3*<sup>Δ/Δ</sup> mice mated with WT male mice. Unpaired two-tailed Student's *t* test. Error bars represent mean  $\pm$  SD \*\*\*,  $P < 0.001$ , NA ( $P > 0.05$ ). **(E)** H&E staining of *Ccnb3*<sup>Δ/Δ</sup> ovaries. The ovary morphology and the number of follicles in *Ccnb3*<sup>Δ/Δ</sup> mice were similar with that in the WT mice. **(F)** The embryos produced by mating *Ccnb3*<sup>Δ/Δ</sup> mice with WT male mice died before E7.5. Bars, 40  $\mu$ m.

meiosis I in *Drosophila* (Jacobs et al., 1998), implying that *Ccnb3* may have a special role in meiotic regulation.

To clarify the function of *Ccnb3* in meiosis in mammalian species, we generated *Ccnb3* mutant mice via CRISPR/Cas9 and found that *Ccnb3* mutation caused female infertility due to the failure of metaphase–anaphase transition in meiosis I. *Ccnb3* was found to be necessary for APC/C activation to initiate anaphase I (Anai), but not required for oocyte maturation, meiosis II progression, or early embryonic development. Our findings may shed light on the differential cell cycle regulatory mechanisms between meiosis and mitosis, as well as between male and female meiosis.

## Results

### *Ccnb3* mutation leads to female infertility

We first detected the expression pattern of *Ccnb3* by quantitative PCR (Q-PCR) and found that its mRNA had a similar expression pattern with *Ccnb1* during oocyte in vitro maturation (IVM), which implied that *Ccnb3* may play an important role in meiosis cell cycle regulation (Fig. 1 A). To study this role of *Ccnb3*, we generated *Ccnb3* mutant mice (referred to as *Ccnb3*<sup>Δ/Y</sup> and *Ccnb3*<sup>Δ/Δ</sup> for male and female mutants, respectively) via CRISPR-mediated deletion of 29 bp in exon 3 of the *Ccnb3* gene located on the X chromosome (Fig. S1 A). The genotypes and protein expression of *Ccnb3* mutant mice were verified by PCR (Fig. 1 B) and Western blot (Fig. 1 C). By natural mating, we found that the *Ccnb3*<sup>Δ/Δ</sup> mice were infertile, while the *Ccnb3*<sup>Δ/Y</sup>

mice showed normal fertility (Fig. 1 D). To find the detailed mechanism of female infertility, we examined ovary development and folliculogenesis in *Ccnb3*<sup>Δ/Δ</sup> female mice. The H&E staining results showed that the *Ccnb3*<sup>Δ/Δ</sup> ovary development was normal (Fig. 1 E), and the number of oocytes superovulated from *Ccnb3*<sup>Δ/Δ</sup> mice was similar to that from WT female mice (referred to as *Ccnb3*<sup>WT/WT</sup>; Fig. S1 B). To investigate whether the infertility was caused by embryonic lethality, we collected embryos from *Ccnb3*<sup>Δ/Δ</sup> female mice with vaginal plugs, after mating with *Ccnb3*<sup>WT/Y</sup> (male WT) mice. All the collected fetuses were degenerated before embryonic day 7.5 (E7.5; Fig. 1 F). These results showed that *Ccnb3* mutation leads to female infertility, while the defects were caused by embryonic lethality rather than abnormal follicular development.

### *Ccnb3* mutation causes oocyte meiotic arrest at metaphase I (MetI)

Although the number of superovulated oocytes from *Ccnb3*<sup>Δ/Δ</sup> mice was identical to those from *Ccnb3*<sup>WT/WT</sup> mice, the first polar body (PB1) was not observed in the *Ccnb3*<sup>Δ/Δ</sup> oocytes (Fig. S1, C and D). We suspected that the defects in *Ccnb3*<sup>Δ/Δ</sup> mice may occur at the time of meiosis progression. To confirm this hypothesis, we analyzed the meiosis maturation process of the *Ccnb3*<sup>Δ/Δ</sup> oocytes using IVM (Fig. 2 A and Fig. S2, A and B) and living cell-tracking assays (Fig. 2 B). We found that the fully grown germinal vesicle (GV)–stage *Ccnb3*<sup>Δ/Δ</sup> oocytes resumed meiosis with successive occurrences of GV breakdown (GVBD) and MetI spindle formation (Fig. 2 C). The efficiency of GVBD of

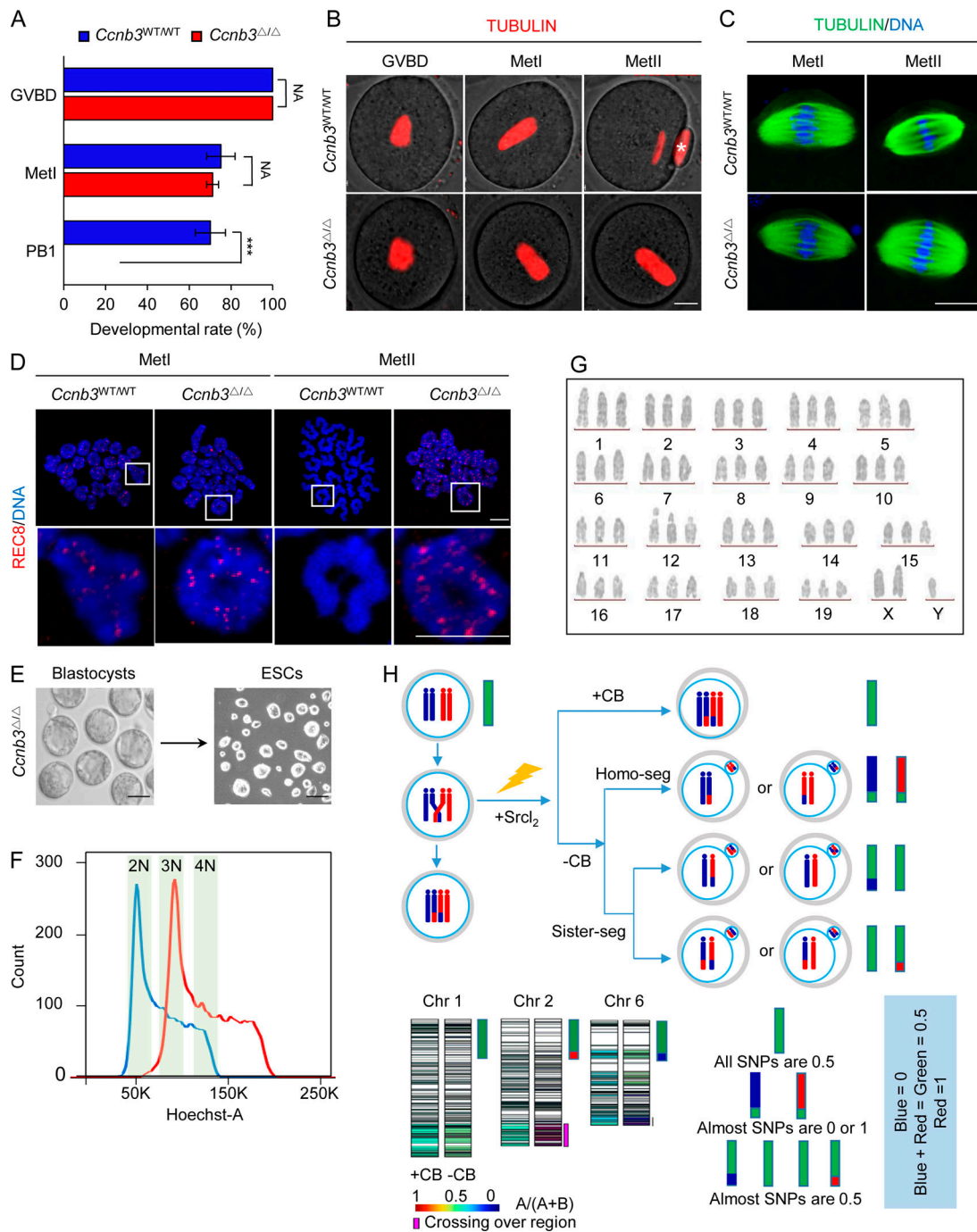


**Figure 2. *Ccnb3* mutation caused mouse oocyte meiotic arrest at MetII. (A)** Oocytes with *Ccnb3* mutation failed to extrude PB1 by IVM assay. Oocytes were incubated in M2 medium to resume meiosis. Oocytes developmental capacity was measured by Hoechst 33342 staining after 0, 6, and 12 h of GVBD, which were represented the GVBD, MetI, and MetII oocyte stage, respectively. The PB1 rate was measured at 8 h after GVBD. At least 100 oocytes were measured in each group. Unpaired two-tailed Student's *t* test. Error bars represent mean  $\pm$  SD. \*\*\*,  $P < 0.001$ , NA ( $P > 0.05$ ). **(B)** WT and *Ccnb3* mutant oocytes cultured for 4 h after GVBD used for living cell tracking to observe spindle formation and PB1 extrusion ( $n = 30$  oocytes per each group). The asterisk indicates the PB1. **(C)** Immunofluorescence staining of tubulin during IVM. At least 30 oocytes were used for immunofluorescence staining. Both WT and *Ccnb3* mutant oocytes showed the metaphase spindle. **(D)** Immunofluorescence staining for the localization of REC8 on chromosomes after *Ccnb3* mutant oocytes at the GVBD stage were cultured for 6 and 12 h ( $n = 40$  oocytes per each group). **(E)** Representative of blastocysts (left) and ESC colonies (right) derived from *Ccnb3*<sup>+/+</sup> oocytes by ICSI. Both blastocysts and ESCs showed normal morphology. **(F)** DNA content analysis of *Ccnb3*<sup>+/+</sup> oocyte-derived ESCs by FACS. The blue peak represents the WT ESCs, which had diploid DNA contents; while the red peak represents the *Ccnb3*<sup>+/+</sup> ESCs, which had triploid DNA contents. 2N, 3N, and 4N represents diploid, triploid, and tetraploid, respectively. **(G)** Karyotype analysis of *Ccnb3*<sup>+/+</sup> oocyte-derived ESCs. The ESCs are triploid with "57 + XXY" karyotype. **(H)** Schematic of chromosome segregation and whole genome sequencing analysis (Chromosomes 1, 2, and 6 are shown) during establishment of *Ccnb3*<sup>+/+</sup> oocyte-derived ESCs by PA. The 4N ESCs (with CB treatment, referred to as +CB) and 2N ESCs (without CB treatment, referred to as -CB) were sequenced separately. Only the heterozygous sites in 4N ESCs and the corresponding sites in 2N ESCs are shown. As calculated by the base frequency ratio in one genome locus, the heterozygous sites are marked ranging from green to blue, the homozygous sites are marked in red or blue and the missing site is blank. The homozygous

regions are inferred as the crossing-over region through the homozygous sites in 2N ESCs. To distinguish that chromosome segregation happens in homologous chromosomes or the sister chromatids, we established two ESCs from *Ccnb3*<sup>+/+</sup> PA embryos, one of which contains 4N chromosomes with no PB extrusion (with CB treatment, referred to as 4N ESCs). The other contains 2N chromosomes with one PB extrusion after PA (without CB treatment, referred to as 2N ESCs). Whole genome DNA sequencing was performed. We defined SNPs as 0 (blue) or 1 (red), so if one SNP point is heterozygous, then its value will be 0.5 (blue + red = green), or else its value will be 0 or 1. Thus, the value for all SNPs in 4N ESCs would be 0.5. If the segregation happened between homozygous chromosomes, almost all SNPs in 2N ESCs would be 0 or 1 and the crossover parts would be 0.5; while if segregation happened between sister chromatids, almost all SNP points would be 0.5, and the crossover parts would be 0 or 1. Bars: 20 μm (B and C); 5 μm (D); 100 μm (E).

*Ccnb3*<sup>+/+</sup> oocytes was equivalent to that of the WT (81.1 vs. 88.5%, respectively; Fig. 2 A). However, a successive blockade in MetI was exclusively generated in *Ccnb3*<sup>+/+</sup> oocytes, failing to extrude PB1 and still maintaining bivalent homologous chromosomes after 10 h of GVBD, when the *Ccnb3*<sup>WT/WT</sup> oocytes had entered the MetII, characterized by visible PB1 and univalent sister chromatids (Fig. 2, B and D). We further observed the REC8 protein, a specific meiotic cohesin and found that REC8 was persistently presented on the chromosome arms with a typical feature of MetI when AnaI was initiated, which indicated that the *Ccnb3*<sup>+/+</sup> oocytes were arrested at MetI with inseparable homologous chromosomes (Fig. 2 D).

#### ***Ccnb3* mutation does not affect preimplantation embryonic development and sister chromatid separation**

To evaluate the effect of *Ccnb3* mutation on the developmental capacity of oocytes, we injected WT sperms into the *Ccnb3*<sup>+/+</sup> oocytes through intracytoplasmic sperm injection (ICSI). Interestingly, fertilized *Ccnb3*<sup>+/+</sup> oocytes were able to extrude the PB and develop into blastocysts (Fig. 2 E) with similar efficiency as those embryos in *Ccnb3*<sup>WT/WT</sup> group (75.6 vs. 80.6%; Table S1), indicating that *Ccnb3* mutation did not affect the preimplantation developmental capacity of embryos. We further established the embryonic stem cell (ESC) lines from these ICSI-derived blastocysts (Fig. 2 E) and analyzed the DNA content and karyotype of the *Ccnb3*<sup>+/+</sup> oocyte-derived ESCs. We found that the *Ccnb3*<sup>+/+</sup> ESCs were triploid and maintained a stable “57 + XXY” karyotype (Fig. 2, F and G). This triploid karyotype may account for the E7.5 degeneration (Fig. 1 F), which was consistent with previous reports (Niemierko, 1981).

As *Ccnb3*<sup>+/+</sup> oocytes can extrude PB after ICSI, we were curious about what kind of PB extrusion occurred in MetI-arrested oocytes after parthenogenetic activation (PA) or ICSI. In other words, the MetI-arrested oocytes may either continue to complete meiosis I by releasing the PB1 or directly skip the meiosis I to complete meiosis II by separating the sister chromatids and releasing the PB2. The genome-wide single nucleotide polymorphism (SNP) analysis on parental chromosomes is feasible for validating the genetic provenance of ESCs, which distinguished the PA-derived ESCs from fertilized ESCs (Kim et al., 2007; Mai et al., 2007). Hence, we analyzed the whole genome SNPs in *Ccnb3*<sup>+/+</sup> PA-derived ESCs to distinguish the homologous chromosome separation from the sister-chromatid separation. There were two types of ESCs established from *Ccnb3*<sup>+/+</sup> PA-embryos, one of which contains tetraploid set of chromosomes due to no PB extrusion by cytochalasin B (CB) treatment (referred to as 4N ESCs) and represents the whole genome SNPs of the CD-1 mice. The other contains diploid set of chromosomes due to one PB extrusion after PA (without CB treatment;

referred to as 2N ESCs), which mimic the PB extrusion of MetI-arrested oocytes after ICSI or PA.

Whole genome DNA sequencing analysis showed that all SNPs in 4N ESCs were heterozygous. While in the 2N ESCs, if the segregation happened between homozygous chromosomes, SNPs would be almost homozygous, and only a fraction of the crossover parts would be heterozygous; and if segregation happened between sister chromatids, SNPs would be almost heterozygous, and only the crossover parts would be homozygous (Fig. 2 H). Our SNP analysis showed that in the 2N ESCs, SNPs were almost heterozygous, and only a fraction of crossover parts was homozygous, which implied that the sister chromatids of *Ccnb3*<sup>+/+</sup> oocytes were separated after PA (Fig. 2 H and Fig. S2 C). In other words, fertilization or PA triggered separation of sister chromatids instead of homozygous chromosomes in *Ccnb3*<sup>+/+</sup> oocytes.

#### ***Ccnb3* mutation induces insufficient APC/C activity with normal SAC dynamics**

To test whether the MetI arrest was due to the insufficiency of APC/C activity in *Ccnb3*<sup>+/+</sup> mice, we traced dynamic changes of the APC/C substrates, Ccnb1 and securin, during IVM by injecting mRNA of Ccnb1-EGFP or securin-EGFP into GV-stage oocytes (Thornton and Toczyski, 2003). The green fluorescence intensity remained almost unchanged during meiosis I progression in the *Ccnb3*<sup>+/+</sup> oocytes, while the WT oocytes experienced a significant decline with PB1 extrusion (Fig. 3, A–D). Securin is known for its role in inactivating the cohesin-cleaving enzyme, separase, until the metaphase–anaphase transition (Marangos and Carroll, 2008). We further confirmed inefficient degradation of endogenous securin protein by immunofluorescence staining (Fig. 3 E). These results indicated that there was no effective APC/C activity for Ccnb1 and securin degradation in *Ccnb3*<sup>+/+</sup> oocytes, and Ccnb3 is necessary for fully activated APC/C to induce the MetI–AnaI transition.

Fully activated APC/C activation requires the satisfaction of SAC (Nilsson et al., 2008). To evaluate the SAC dynamic changes during meiosis I, we detected the SAC proteins, BUB3 and MAD2, by immunofluorescence (Homer et al., 2005a,b; Li et al., 2009). Both BUB3 and MAD2 were deprived from the kinetochores during the pro-MetI to MetI transition, both in the WT and *Ccnb3*<sup>+/+</sup> oocytes (Fig. 3 F and Fig. S3 A), which suggested that *Ccnb3* mutation does not affect the normal function of SAC.

#### **Reducing securin or CDK1 activity rescues the defects of MetI arrest**

As *Ccnb3* mutation leads to feeble degradation of both Ccnb1 and securin at the beginning of anaphase, we wanted to confirm whether direct interference with APC/C substrates in MetI

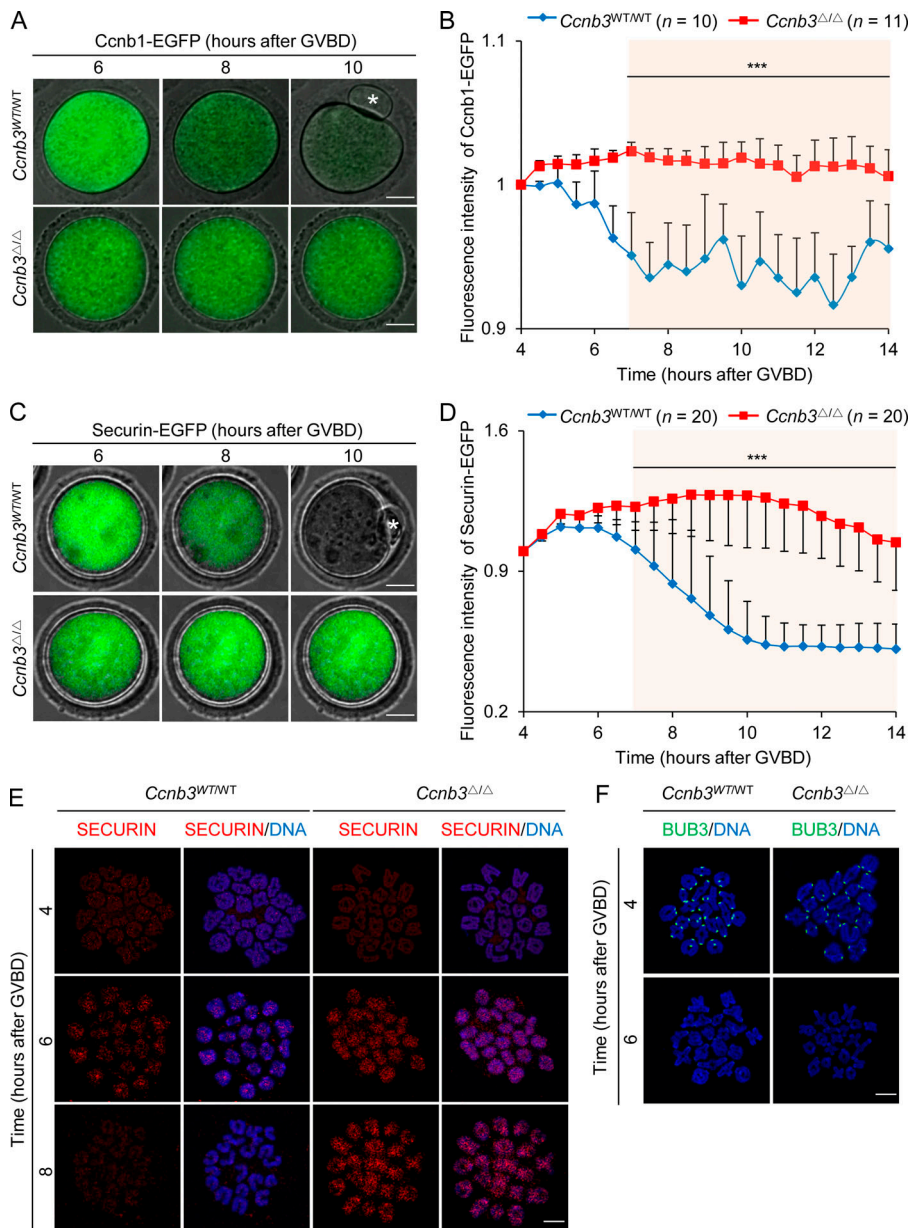


**Figure 3. *Ccnb3* mutation with inefficient APC/C activity and functional SAC. (A–D)** Time-lapse fluorescence measurement of *Ccnb1*-EGFP (A and B) and securin-EGFP (C and D) expressed of indicated mRNA injection at GV stage, respectively. The integrated intensities of EGFP were measured, background corrected, and normalized to the initial-intensity value obtained per oocyte. GV-stage oocytes were injected with 100 ng/μl *Ccnb1*-EGFP or securin-EGFP mRNA, incubated in M2 medium containing dbcAMP-free M2 medium to resume meiosis. At least 10 and 20 oocytes for *Ccnb1*-EGFP and securin-EGFP were tested, respectively. Measurements were aligned to 4 h after GVBD as the starting time. The asterisk indicates the PB1. Statistical analyses for differential securin-GFP fluorescence intensity changes. Error bars represent mean ± SD; \*\*\*, P < 0.001 (Student's *t* test). **(E)** Chromosome spreads were prepared 4 h (pro-MetI), 6 h (MetI), and 8 h (AnaI) after GVBD and then stained with SECURIN (red) and Hoechst 33342 (blue). **(F)** Chromosome spreads were prepared 4 h (pro-MetI) and 6 h (MetI) after GVBD, then stained with BUB3 (green) and Hoechst 33342 (blue). Bars: 20 μm (A and C); 5 μm (E and F).

could rescue the phenotype of *Ccnb3*-deficient oocytes. We knocked down *Ccnb1* and securin by injecting corresponding siRNA into GV-stage oocytes, respectively (Fig. S3 B). Surprisingly, knocking down either of them did not affect the development rate of GVBD (Fig. S3 C), while only reducing securin could restore the PB1 extrusion of *Ccnb3<sup>Δ/Δ</sup>* oocytes (Fig. 4, A and B). As CDK1 activity in the *Ccnb3* mutant oocytes is significantly higher at AnaI (10 h after GVBD; Fig. S3 D), we tried to interfere with pan-CDK1 activity at MetI (6 h after GVBD) using the small molecule inhibitor, RO-3306. As expected, acute pharmacological inhibition of CDK1 partially rescued MetI arrest caused by *Ccnb3* mutation and led to the PB1 extrusion (Fig. S3 E).

Our results collectively show that *Ccnb3* mutant oocytes could not fully activate the APC/C and decline the CDK1 activity, which led to the failure of AnaI onset. Knockdown of securin or inhibition of CDK1 activity could rescue these defects. Securin and CDK1 worked synergistically to regulate the activity of separase,

which cleaves the cohesin complexes to dissolve homologous chromosomes and sister chromatid at anaphase onset in meiosis and mitosis (Gorr et al., 2005; Stemmann et al., 2006). These findings indicated that *Ccnb3* functioned to fully activate the APC/C to activate separase during MetI–AnaI transition by declining securin and CDK1 activity, resulting in a triumphant AnaI onset.

#### ***Ccnb3* replenishment recovers the deficiency of MetI arrest**

To investigate whether *Ccnb3* protein could recover the MetI arrest in *Ccnb3<sup>Δ/Δ</sup>* oocytes, we injected *Ccnb3* mRNA into *Ccnb3<sup>Δ/Δ</sup>* oocytes at GV stage (Fig. S3 F). Our results showed that replenishment of *Ccnb3* mRNA could reverse the *Ccnb3* mutant phenotypes by recovering PB1 extrusion (Fig. 4 C). The recovered PB1 extrusion, characterized by homologous chromosome separation and disappearance of bivalent chromosomes, was confirmed by chromosome spread assay (Fig. 4 D). Moreover,

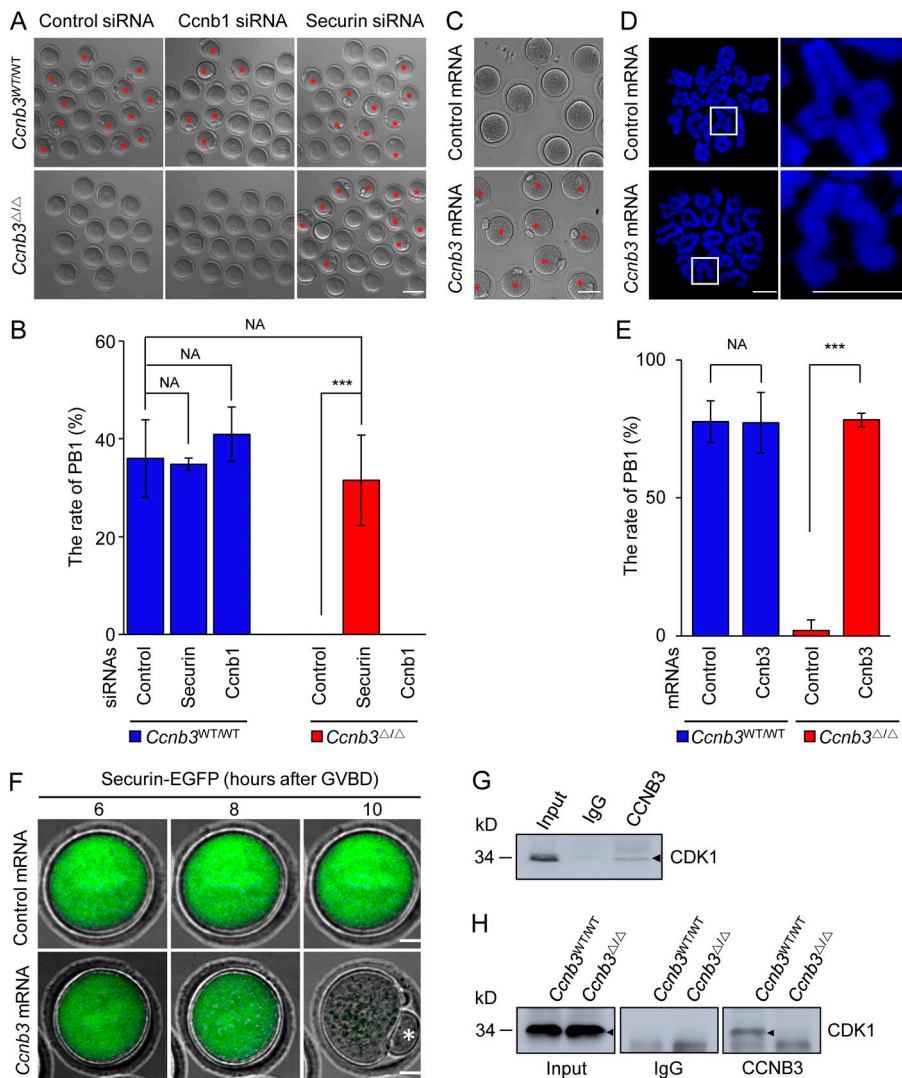


**Figure 4. APC/C activity was indispensable for MetI-Anal transition in oocytes. (A and B)** *Ccnb3*<sup>Δ/Δ</sup> oocytes injected with the indicated siRNAs, entered into meiosis I, qualitatively (A) and quantitatively (B) determined by PB extrusion. siRNAs were injected into at least 50 oocytes in each group, three repeats. The asterisk indicates PB. Error bars represent mean ± SD; \*\*\*, P < 0.001, NA (P > 0.05; Student's *t* test). **(C)** *Ccnb3*<sup>Δ/Δ</sup> oocytes injected with *Ccnb3* mRNA restored PB extrusion. The asterisk marks PB1. **(D)** Chromosome spreads were prepared and stained with Hoechst 33342 (blue) after *Ccnb3* mRNA injection. *Ccnb3*<sup>Δ/Δ</sup> oocytes had entered to MetII with univalent sister chromatids after *Ccnb3* mRNA injection. At least 80 oocytes were measured. **(E)** The efficiency of PB extrusion was rescued by *Ccnb3* mRNA injection. At least 150 oocytes per group. Error bars represent mean ± SD; \*\*\*, P < 0.001, NA (P > 0.05; Student's *t* test). **(F)** Time-lapse fluorescence measurement of securin-EGFP after *Ccnb3* mRNA injection. The asterisk indicates the PB. **(G)** Representation of IP showing the interaction between CCNB3 and CDK1 using 293T cells with coexpression of mouse *Ccnb3* and CDK1. Metaphase-arrested cells prepared by combining nocodazole (200 ng/ml) and MG132 (5 μM) were collected for IP assay. Anti-CCNB3 was used for IP. **(H)** IP detected the interaction of CCNB3 and CDK1 from testes derived from *Ccnb3*<sup>WT/Y</sup> and *Ccnb3*<sup>Δ/Y</sup> mice. Anti-CCNB3 was used for IP. Bars: 100 μm (A and C); 5 μm (D); 20 μm (F).

the rescued efficiency of PB1 release is comparable to that of the WT (Fig. 4 E), which further indicates the irreplaceable role of *Ccnb3* in meiosis I. The APC/C activity in *Ccnb3*-rescued oocytes was further detected by tracing changes in fluorescence with exogenous injection mRNA of securin-EGFP. Securin protein was quickly degraded in time at the MetI-Anal transition in *Ccnb3* rescued oocytes (Fig. 4 F). These results suggest that *Ccnb3* helps to fully activate the APC/C activity and promote the MetI-Anal transition and PB1 extrusion.

### CCNB3 has direct interactions with CDK1

As cyclins usually collaborate with CDKs to ensure precise operation of the cell cycle (Kishimoto, 2003; Brunet and Maro, 2005; Satyanarayana and Kaldis, 2009), we speculated that CCNB3 may work as a ligand combined with CDKs, like other cyclins. To explore the functional partner of CCNB3, we detected the interaction between CCNB3 and CDK1 by immunoprecipitation (IP) in cells coexpressing the two proteins, confirming that CCNB3 did interact with CDK1 (Fig. 4 G). We further confirmed this result strictly by testing endogenous protein interactions in *Ccnb3*<sup>WT/Y</sup> and *Ccnb3*<sup>Δ/Y</sup> testicular tissue, which

showed CDK1 had interacted with CCNB3 in *Ccnb3*<sup>WT/Y</sup>, but had no interaction in *Ccnb3*<sup>Δ/Y</sup> testicular tissue (Fig. 4 H).

### Discussion

Cyclins play different roles in regulation of male and female meiosis. The infertility of female mice and contrasting fertility of male mice, both with *Ccnb3* mutations, suggested that *Ccnb3* only functioned in females meiosis, which may be related to the long duration of female meiosis I (Gemzell, 1962) and reflected different meiotic regulation mechanisms between the two sexes. Another possibility is that other sexual tendentious cyclins may compensate for the function of *Ccnb3* in males, for instance, cyclin A1. Cyclin A1 is a male-specific cyclin in mice, and its deletion leads to a blocked spermatogenesis before the first meiotic division, whereas female mice remain normal following its deletion (Liu et al., 1998). Nonetheless, the gender bias of cyclins in meiotic regulation is unique, which needs to be further explored.

Successfully execution of metaphase-anaphase transition in eukaryotic cell division requires metaphase cyclins scheduled

degradation at different times, especially cyclin B. Our findings that Ccnb3 played an essential role for MetI-AnaI transition during female meiosis I are consistent with the results in *Drosophila* (Yuan and O'Farrell, 2015) and *Caenorhabditis elegans* (Tarailo-Graovac and Chen, 2012), which implies that the specific role of Ccnb3 in female meiosis is conserved. We also found that knockdown of Ccnb1 without blocking GVBD could not recover the defects in oocytes lacking Ccnb3. A previous report showed that oocyte-specific knockout of Ccnb1 may lead to compensatory increasing of Ccnb2 with normally GVBD occurrence (Li et al., 2018). We speculated that Ccnb2 or cyclin A2 (Murphy et al., 1997) may complement Ccnb1 for maintaining high CDK1 activity to initiate GVBD and block the AnaI onset in oocytes lacking Ccnb3.

Beyond expectation, fertilization or PA directly switched the MetI-arrested oocytes into a fertilized status with PB2 instead of PB1 extrusion. How the spindle accomplishes assembly in the MetI-arrested oocytes will be an interesting question to study further. We verified the normal separation of sister chromatids in Ccnb3<sup>+/Δ</sup> oocytes after activation and the preimplantation developmental capacity of fertilized Ccnb3<sup>+/Δ</sup> oocytes have no defects, which implied that Ccnb3 is a meiosis-specific cyclin required for meiosis I, rather than meiosis II. In addition, the genome-wide SNP analysis provides a reliable application for analyzing the pattern of chromosome segregation.

Previous reports showed that mitotic CDKs phosphorylated APC/C subunits, which is required to allow APC activation by Cdc20 (Rudner and Murray, 2000; Chang et al., 2015). Combined with the above results, we speculated that Ccnb3 binding to CDK1 may function as a kinase which is necessary for full activation of APC/C by directly phosphorylating securin or other APC/C subunits for their timely degradation at AnaI onset. Securin is an inhibitor of separase, and we found that knockdown of securin recovered the MetI arrest in Ccnb3 mutant oocytes. Down-regulation of securin liberated separase, which may directly cleavage of cohesin to separate homologous chromosome. It has been reported that separase acts as repressor of CDK1/cyclin B, which inactivates MPF to ensure anaphase, progress in both mitosis and meiosis I (Gorr et al., 2005, 2006; Shindo et al., 2012). Meanwhile, both separase liberation and CDK1 inactivation may account for the resumption of MetI arrest in Ccnb3 mutant oocytes after securin knockdown, for which a concrete mechanism needs to be further explored. Besides, the meiosis-specific REC8, which is phosphorylated by different kinases (Alexandru et al., 2001; Lee and Amon, 2003; Yu and Koshland, 2005; Katis et al., 2010) to facilitate cohesin to cleavage from chromosomes, persistently remained on the homologous chromosome arm in Ccnb3<sup>+/Δ</sup> oocytes, which implies CCNB3/CDK1 complex may serve as an undiscovered candidate kinase for phosphorylation of REC8.

In this study, we found that Ccnb3 mutation caused female mouse infertility with the failure of metaphase-anaphase transition in oocyte meiosis I, while the Ccnb3 mutant male mice had normal fertility. Oocytes lacking Ccnb3 are characteristic of insufficient APC/C activation and normal preimplantation capacity after fertilization. Meanwhile, we found that Ccnb3 directly interacts with CDK1, which may exert an essential kinase

activity to separate homologous chromosomes. Although we have elucidated the unique role of Ccnb3 in female meiosis, the direct target of Ccnb3 have not been found yet. The core regulatory machinery of Ccnb3 in metaphase to anaphase transition seems to be various in female and male meiosis. Similar findings were obtained independently with a different targeted mutation in Ccnb3 (Karasu et al., 2019). Our study reveals that Ccnb3 serve as a female meiosis-specific cyclin for metaphase-anaphase transition in meiosis I, which opens an avenue to elucidate the unique cell cycle regulation mechanisms for meiosis in mammals. The specific target of Ccnb3 need to be further studied to unraveling the differences of cyclins in female and male meiotic regulation.

## Materials and methods

### Experimental animals

Specific pathogen free-grade mice were obtained from Beijing Vital River Laboratories and housed in the animal facilities of the Chinese Academy of Sciences. All animal studies were performed in accordance with the Guidelines for the Use of Animals in Research issued by the Institute of Zoology, Chinese Academy of Sciences. The mice used in this study were CD-1 strains, and genome editing was performed by CRISPR/Cas9. Six sgRNAs were designed for targeting different sites of the mouse Ccnb3 gene (sgRNA-Ccnb3-1~6). The efficiency of sgRNAs was verified by mouse fibroblast cell transfection, cell sorting, subsequent PCR identification, T7 endonuclease I (T7EI) assay, and Sanger sequencing. SgRNA-Ccnb3-1 showed the highest mutation ratio (12:20; 60%) according to T7 EI and Sanger sequencing, which was selected for in vitro transcription and injection. The injection concentration by ICSI of Cas9 mRNA/sgRNA-Ccnb3-1 was 100:50 ng/μl. The biallelic mutations of Ccnb3 in mouse embryos were produced with relatively high efficiency via zygote injection. Finally, we screened out the Δ29 bp mice for the next experiment. All sgRNAs are listed in Table S2.

### RNA extraction and Q-PCR

Total RNA was extracted with TRIzol reagent (Invitrogen, 15596-018) from 20 oocytes in each group. Q-PCR was performed with Thunderbird SYBR qPCR Mix (Toyobo), using total cDNA as the template, in a total volume of 20 μl, including the primer, and ROX (Toyobo). The thermal cycling conditions of conventional real-time PCR were 1 min at 95°C, followed by 45 cycles of 15 s at 95°C, 15 s at 60°C, and 45 s at 72°C, and the melting curve conditions were 1 min at 95°C, 30 s at 60°C, and 30 s at 95°C. All reactions were performed using an Agilent Technologies Stratagene Mx3005P Real-Time PCR System (Applied Biosystems). Relative gene expression was analyzed based on the 2-ΔΔCt method with Actin as internal control. At least three independent experiments were analyzed. All primers are listed in Table S2.

### Histological analysis

Ovaries from WT and Ccnb3 mutant female mice were fixed in 4% paraformaldehyde at room temperature, overnight. The ovaries were dehydrated stepwise through an ethanol series (70,

80, 90, and 100% ethanol) and processed for paraffin embedding. 5- $\mu$ m sections were cut with a Leica slicing machine (Leica Biosystems, RM2235) and mounted on poly-D-lysine-coated glass slides (Zhong Shan Golding Bridge Biotechnology). After dewaxing and hydration, the sections were stained with H&E, using standard methods and imaged with a Leica Aperio VERSA 8 microscope (Leica Biosystems).

### Collection and culture of oocytes

We isolated GV stage oocytes from minced ovaries of 8–10-wk-old CD-1 female mice. For the *in vivo* method, oocytes collected after injection of 7.5 international units (IU) of pregnant mare's serum gonadotropin, followed by 7.5 IU human chorionic gonadotropin. For the *in vitro* method, GV oocytes were superovulated from adult mice by injection of 7.5 IU pregnant mare's serum gonadotropin after 44 h and cultured *in vitro*. The number of oocytes with PB1 at 8 h after GVBD when the PB1 had just been released. Oocytes were cultured in M2 medium for at least 12 h. The culture was conducted in an incubator under environmental conditions of 5% CO<sub>2</sub>, 37°C, and saturated humidity. To evaluate the developmental capacity of oocytes, oocytes were stained with Hoechst 33342 at different time during *in vitro* culture. For the rescue experiment, oocytes were cultured in media containing RO-3306 at different concentrations and for different lengths of time as indicated in the figure legends.

### Time-lapse confocal microscopy of live oocytes

The fluorogenic, cell-permeable reagent SiR-Tubulin (Cytoskeleton, CY-SC002) was used to image tubulin in living cells. GV-stage oocytes were injected with 10  $\mu$ l of 100 ng/ $\mu$ l mRNA encoding securin-EGFP in M2 medium containing 250 mM dbcAMP using methods described elsewhere (Jaffe and Terasaki, 2004). Following mRNA injection, oocytes were cultured for 2–3 h at 37°C to allow securin-EGFP expression. Oocytes were cultured in dbcAMP-free M2 medium placed in a European Molecular Biology Laboratory environmental microscope incubator (GP106), allowing cells to be maintained in a 5% CO<sub>2</sub> atmosphere at 37°C with humidity control during imaging. Time-lapse image acquisitions were performed using a customized Zeiss LSM510 META confocal microscope equipped with a 532-nm excitation laser, a long-pass 545-nm emission filter, a 403 C-Apochromat 1.2 NA water immersion objective lens, and an in-house developed 3D tracking macro (Rabut and Ellenberg, 2004).

### Preparation and staining of chromosome spreads

Chromosome spreads of mouse oocytes during meiotic maturation were prepared using methods previously described (Hodges and Hunt, 2002). Oocytes were briefly exposed to acid Tyrode's solution (Sigma) to remove the zona pellucida under the microscope to avoid overdigestion. After a brief recovery in M2 medium, the oocytes were transferred onto glass slides and fixed in a solution of 1% paraformaldehyde in distilled H<sub>2</sub>O (pH 9.2) containing 0.15% Triton X-100 and 3 mM dithiothreitol. The dried chromosome spreads were stained with 10  $\mu$ g/ml Hoechst 33342 for DNA counterstaining, following immunofluorescence

staining when required. The slides were dried slowly in a humidified chamber for several hours and then blocked with 2% BSA in PBS for 1 h at room temperature or overnight at 4°C and incubated with primary antibodies overnight at 4°C. After brief washes with washing buffer, the slides were then incubated with corresponding secondary antibodies for 1 h at room temperature. Rabbit anti-REC8 antibody (Abcam, ab192241) for marking homologous chromosomes was used as the primary antibody, and appropriate secondary antibody conjugated with Alexa Fluor Cy3 (Invitrogen) was used. The samples were observed under a laser-scanning confocal microscope (Zeiss LSM 780).

### *Ccnb3*<sup>-/-</sup> ESCs derivation and cell culture

CD-1 mouse blastocysts were used to derive ESCs. The culture medium composed of N2B27 medium (Gibco), 1 mM L-glutamine, 0.1 mM  $\beta$ -mercaptoethanol, 50 U/ml penicillin, 50  $\mu$ g/ml streptomycin, 3  $\mu$ M CHIR99021 (Stemgent), 1  $\mu$ M PD0325901 (Stemgent), and mLIF (ESGRO). The embryos were incubated at 37°C in a 5% CO<sub>2</sub> incubator for 4–5 d, and then the formed outgrowths (named passage 0) were picked separately using a glass pipette and dissociated with 0.25% trypsin-EDTA solution (Gibco). The cells were replanted and survived from the first trypsinization of the outgrowth were counted as passage 1. For routine passage, the passage ratio was ~1:8, and mouse ESCs were passaged around every 3 d.

### DNA content analysis of *Ccnb3*<sup>-/-</sup> ESCs

*Ccnb3*<sup>-/-</sup> ESCs were purified and analyzed by FACS. Single-cell suspensions were obtained by trypsin-EDTA digestion and repetitive pipetting and sieved through a 40- $\mu$ m cell strainer. Cells were incubated with 10  $\mu$ g/ml Hoechst 33342 (Invitrogen, H3570) for 15–20 min at 37°C before analysis. Data were collected with MoFlo XDP cell sorter (Beckman-Coulter). *Ccnb3*<sup>WT/WT</sup> ESCs (2N) were used as a control.

### Karyotype analysis of *Ccnb3*<sup>-/-</sup> ESCs

*Ccnb3*<sup>-/-</sup> ESCs were incubated with 0.2 mg/ml nocodazole (Sigma, M1404) for 3 h. After trypsinization, the ESCs were suspended in 0.075 M KCl at 37°C for 30 min. Then, the cells were fixed in solution consisting of methanol and acetic acid (3:1 in volume) for 30 min and then were dropped onto precleaned slides. The cells were stained with Giemsa stain (Sigma, GS500ML) for 15 min after being incubated in 5 M HCl. More than 30 metaphase spreads were analyzed.

### DNA sequencing of *Ccnb3* PA-derived ESCs

Collected oocytes were parthenogenetic activated in Ca<sup>2+</sup>-free CZB (Chatot Ziomek Bavister medium) containing 10 mM Sr<sup>2+</sup> with (5 nM) and without CB for 6 h. PA-embryos were used to establish ESCs. Two ESCs from *Ccnb3*<sup>-/-</sup> PA-embryos were established, one of which contained 4N chromosomes with no PB extrusion (+CB, 4N ESCs) and the other containing 2N chromosomes with one PB extrusion after PA (-CB, 2N ESCs). At least 10<sup>7</sup> ESCs were collected for DNA sequencing. DNA was isolated and checked using the Nano Photometer Spectrophotometer and Qubit 2.0 Fluorometer and 1  $\mu$ g DNA template



according to TruSeq DNA Sample Preparation Guide (Illumina, 15026486 Rev.C) method and process for library preparation. The Illumina HiSeq X Ten, PE150 strategy was used for sequencing the identified library. The clean reads were mapped to the mouse reference genome (mm9) using a Burrows-Wheeler Aligner (version 0.7.15; [Rabut and Ellenberg, 2004](#)). After removing duplicated reads, the base distribution for each chromosomal location was calculated using the Pysamstats (version 1.0.0), developed by A. Miles (University of Oxford, Oxford, England, UK). The single nucleotide variations in 4N ESCs sample with >10× coverage were used for the SNP identification. Sites selected for analysis were covered by two types of bases, located within nonrepeat genome regions (RepeatMasker, Institute for Systems Biology). Then, the sites with minor base taking >30% reads were used for the analysis. Next, we calculated the corresponding base frequency distribution in the 2N ESCs sample. During the homologous chromosome separation, the 2N ESCs sample showed the homozygous state in the identified single nucleotide variations sites; whereas, the cell showed sister chromatid separation and the homologous chromosomes were retained.

#### Immunofluorescence analysis

Oocytes were first fixed in 4% paraformaldehyde at room temperature for 30 min and then permeabilized in PBS containing 0.5% Triton X-100 for 20 min. Next, oocytes were blocked in PBS with 2% BSA for 1 h and then incubated with FITC- $\alpha$ -tubulin (Sigma, F2618) primary antibody at room temperature for 1 h. After washing three times with PBS, DNA was stained with Hoechst 33342. The samples were then mounted on slides and were observed under a laser-scanning confocal microscope (Zeiss LSM 780). At least 40 oocytes were examined in each treatment, and each treatment was repeated three times. All antibodies used in this study are listed in the Table S3.

#### IP and Western blotting

Magnetic Beads Protein G were coated with 5  $\mu$ g of the primary antibody in IP wash buffer (50 mM Tris-HCl, pH 7.4, 150 mM sodium chloride, 1 mM MgCl<sub>2</sub>, and 0.05% NP-40) containing 5% BSA overnight with rotation at 4°C. Then, we collected mouse testes or specific cells and added IP lysis buffer (150 mM NaCl, 50 mM Tris-HCl, pH 7.4, 1 mM EDTA, 0.1% SDS, 1% NP-40, 0.5% sodium deoxycholate, 0.5 mM DTT, and 1 mM PMSF/cocktail) followed by incubation on ice for 10 min. Next, we centrifuged the IP lysate at 14,000 rpm for 10 min at 4°C, removed 100  $\mu$ l of the supernatant and added this to 900  $\mu$ l of the beads-antibody complex in IP Buffer (860  $\mu$ l IP wash buffer and 35  $\mu$ l 0.5 M EDTA) and incubated this with rotation overnight at 4°C. After washing, 50  $\mu$ l elution buffer was added to the immunoprecipitate and the supernatant was used for Western blot. Western blotting was performed as described previously ([Wu et al., 2005](#)). The commercial antibodies used were anti-CDK1 (Abcam, ab32094) and anti-cyclin B3 (C517).

#### MPF concentration assay

MPF concentration was measured by using mouse MPF assay ELISA kit (JiangLai Biology) according to the manufacturer's

instruction. In brief, cell lysates were added into the purified HRP-labeled cyclin B and CDK1 antibodies to form the antibody-antigen-enzyme-antibody complexes, and the complexes were catalyzed by HRP enzyme. After adding the tetramethylbenzidine substrate solution, MPF concentration was determined by measuring the absorbance of converted dye at a wavelength of 450 nm.

#### Statistical analysis

Statistical parameters including statistical analysis, statistical significance, and *n* value are reported in the figure legends. Statistical analyses were performed using Prism Software (GraphPad). For statistical comparison, Student's *t* test was used. A value of *P* < 0.05 was considered significant, and NA stands for significant difference is not available with *P* > 0.05.

#### Online supplemental material

Fig. S1 describes the characters of *Ccnb3* mutant mice. Fig. S2 shows the development of *Ccnb3* mutant oocytes in meiosis. Fig. S3 exhibits the rescue of MetI arrest caused by *Ccnb3* mutation. Table S1 shows the developmental capacity of *Ccnb3*<sup>Δ/Δ</sup> oocytes after ICSI. Table S2 lists the sgRNAs and primers designed in the study. Table S3 lists the reagent and resource used in the study.

#### Acknowledgments

We thank Scott Keeney (Howard Hughes Medical Institute; Memorial Sloan-Kettering Cancer Center) and Katja Wassmann (Sorbonne Université, Institut de Biologie Paris Seine) for generously sharing unpublished data and antibody information. We thank Lijuan Wang for assistance with live cell imaging; Shiwen Li and Xili Zhu for assistance with immunofluorescent staining; and Ming Ge for the microinjection of GV oocytes.

This study was supported by the National Key Research and Development Program (2017YFA0103803 and 2018YFC1004500), the China National Postdoctoral Program for Innovative Talents (BX201700243 to L. Wang), the National Natural Science Foundation of China (31621004 and 81571356 to Q. Zhou), and Key Research Projects of the Frontier Science of the Chinese Academy of Sciences (QYZDY-SSW-SMC002 to Q. Zhou).

The authors declare no competing financial interests.

W. Li, Q. Zhou, and Y. Zhang conceived and designed the experiments; L. Wang performed the ICS with the help of C. Liu and H. Sun; L. Zhang performed the Q-PCR, genotyping, and Western blot, with the help of J. Han and P. Li; G. Feng and J. Mao analyzed the DNA sequencing data; other experiments and analysis were performed by Y. Li and Z. He, with the help of X. Yuan and L. Jiang; J. Wang and Z. Li provided insightful suggestions for the manuscript and preparation. Y. Li wrote the manuscript with the help of other authors.

Submitted: 14 August 2018

Revised: 18 December 2018

Accepted: 7 February 2019

## References

- Alexandru, G., F. Uhlmann, K. Mechtler, M.A. Poupard, and K. Nasmyth. 2001. Phosphorylation of the cohesin subunit Scc1 by Polo/Cdc5 kinase regulates sister chromatid separation in yeast. *Cell*. 105:459–472. [https://doi.org/10.1016/S0092-8674\(01\)00362-2](https://doi.org/10.1016/S0092-8674(01)00362-2)
- Brandeis, M., I. Rosewell, M. Carrington, T. Crompton, M.A. Jacobs, J. Kirk, J. Gannon, and T. Hunt. 1998. Cyclin B2-null mice develop normally and are fertile whereas cyclin B1-null mice die in utero. *Proc. Natl. Acad. Sci. USA*. 95:4344–4349. <https://doi.org/10.1073/pnas.95.8.4344>
- Brunet, S., and B. Maro. 2005. Cytoskeleton and cell cycle control during meiotic maturation of the mouse oocyte: integrating time and space. *Reproduction*. 130:801–811. <https://doi.org/10.1530/rep.1.00364>
- Chang, L., Z. Zhang, J. Yang, S.H. McLaughlin, and D. Barford. 2015. Atomic structure of the APC/C and its mechanism of protein ubiquitination. *Nature*. 522:450–454. <https://doi.org/10.1038/nature14471>
- Gallant, P., and E.A. Nigg. 1994. Identification of a novel vertebrate cyclin: cyclin B3 shares properties with both A- and B-type cyclins. *EMBO J.* 13: 595–605. <https://doi.org/10.1002/j.1460-2075.1994.tb06297.x>
- Gemzell, C.A. 1962. Induction of ovulation with human pituitary gonadotrophins. *Fertil. Steril.* 13:153–168. [https://doi.org/10.1016/S0015-0282\(16\)34445-4](https://doi.org/10.1016/S0015-0282(16)34445-4)
- Gorr, I.H., D. Boos, and O. Stemmann. 2005. Mutual inhibition of separase and Cdk1 by two-step complex formation. *Mol. Cell*. 19:135–141. <https://doi.org/10.1016/j.molcel.2005.05.022>
- Gorr, I.H., A. Reis, D. Boos, M. Wühr, S. Madgwick, K.T. Jones, and O. Stemmann. 2006. Essential CDK1-inhibitory role for separase during meiosis I in vertebrate oocytes. *Nat. Cell Biol.* 8:1035–1037. <https://doi.org/10.1038/ncb1467>
- Hodges, C.A., and P.A. Hunt. 2002. Simultaneous analysis of chromosomes and chromosome-associated proteins in mammalian oocytes and embryos. *Chromosoma*. 111:165–169. <https://doi.org/10.1007/s00412-002-0195-3>
- Homer, H.A., A. McDougall, M. Levasseur, A.P. Murdoch, and M. Herbert. 2005a. Mad2 is required for inhibiting securin and cyclin B degradation following spindle depolymerisation in meiosis I mouse oocytes. *Reproduction*. 130:829–843. <https://doi.org/10.1530/rep.1.00856>
- Homer, H.A., A. McDougall, M. Levasseur, K. Yallop, A.P. Murdoch, and M. Herbert. 2005b. Mad2 prevents aneuploidy and premature proteolysis of cyclin B and securin during meiosis I in mouse oocytes. *Genes Dev.* 19: 202–207. <https://doi.org/10.1101/gad.328105>
- Jacobs, H.W., J.A. Knoblich, and C.F. Lehner. 1998. Drosophila Cyclin B3 is required for female fertility and is dispensable for mitosis like Cyclin B. *Genes Dev.* 12:3741–3751. <https://doi.org/10.1101/gad.12.23.3741>
- Jaffe, L.A., and M. Terasaki. 2004. Quantitative microinjection of oocytes, eggs, and embryos. *Methods Cell Biol.* 74:219–242. [https://doi.org/10.1016/S0091-679X\(04\)74010-8](https://doi.org/10.1016/S0091-679X(04)74010-8)
- Jones, K.T. 2004. Turning it on and off: M-phase promoting factor during meiotic maturation and fertilization. *Mol. Hum. Reprod.* 10:1–5. <https://doi.org/10.1093/molehr/gah009>
- Karasu, M.E., N. Bouftas, S. Keeney, and K. Wassmann. 2019. Cyclin B3 promotes anaphase I onset in oocyte meiosis. *J. Cell Biol.* <https://doi.org/10.1083/jcb.201808091>
- Katis, V.L., J.J. Lipp, R. Imre, A. Bogdanova, E. Okaz, B. Habermann, K. Mechtler, K. Nasmyth, and W. Zachariae. 2010. Rec8 phosphorylation by casein kinase 1 and Cdc7-Dbf4 kinase regulates cohesin cleavage by separase during meiosis. *Dev. Cell*. 18:397–409. <https://doi.org/10.1016/j.devcel.2010.01.014>
- Kim, K., K. Ng, P.J. Rugg-Gunn, J.H. Shieh, O. Kirak, R. Jaenisch, T. Wakayama, M.A. Moore, R.A. Pedersen, and G.Q. Daley. 2007. Recombination signatures distinguish embryonic stem cells derived by parthenogenesis and somatic cell nuclear transfer. *Cell Stem Cell*. 1: 346–352. <https://doi.org/10.1016/j.stem.2007.07.001>
- Kishimoto, T. 2003. Cell-cycle control during meiotic maturation. *Curr. Opin. Cell Biol.* 15:654–663. <https://doi.org/10.1016/j.ceb.2003.10.010>
- Lee, B.H., and A. Amon. 2003. Role of Polo-like kinase CDC5 in programming meiosis I chromosome segregation. *Science*. 300:482–486. <https://doi.org/10.1126/science.1081846>
- Li, J., J.X. Tang, J.M. Cheng, B. Hu, Y.Q. Wang, B. Aalia, X.Y. Li, C. Jin, X.X. Wang, S.L. Deng, et al. 2018. Cyclin B2 can compensate for Cyclin B1 in oocyte meiosis I. *J. Cell Biol.* 217:3901–3911. <https://doi.org/10.1083/jcb.201802077>
- Li, M., S. Li, J. Yuan, Z.B. Wang, S.C. Sun, H. Schatten, and Q.Y. Sun. 2009. Bub3 is a spindle assembly checkpoint protein regulating chromosome segregation during mouse oocyte meiosis. *PLoS One*. 4:e7701. <https://doi.org/10.1371/journal.pone.0007701>
- Liu, D., M.M. Matzuk, W.K. Sung, Q. Guo, P. Wang, and D.J. Wolgemuth. 1998. Cyclin A1 is required for meiosis in the male mouse. *Nat. Genet.* 20: 377–380. <https://doi.org/10.1038/3855>
- Lozano, J.C., E. Perret, P. Schatt, C. Arnould, G. Peaucellier, and A. Picard. 2002. Molecular cloning, gene localization, and structure of human cyclin B3. *Biochem. Biophys. Res. Commun.* 291:406–413. <https://doi.org/10.1006/bbrc.2002.6458>
- Mai, Q., Y. Yu, T. Li, L. Wang, M.J. Chen, S.Z. Huang, C. Zhou, and Q. Zhou. 2007. Derivation of human embryonic stem cell lines from parthenogenetic blastocysts. *Cell Res.* 17:1008–1019. <https://doi.org/10.1038/cr.2007.102>
- Marangos, P., and J. Carroll. 2008. Securin regulates entry into M-phase by modulating the stability of cyclin B. *Nat. Cell Biol.* 10:445–451. <https://doi.org/10.1038/ncb1707>
- Murphy, M., M.G. Stinnakre, C. Senamaud-Beaufort, N.J. Winston, C. Sweeney, M. Kubelka, M. Carrington, C. Bréchet, and J. Sobczak-Thépot. 1997. Delayed early embryonic lethality following disruption of the murine cyclin A2 gene. *Nat. Genet.* 15:83–86. <https://doi.org/10.1038/ng0197-83>
- Nguyen, T.B., K. Manova, P. Capodiceci, C. Lindon, S. Bottega, X.Y. Wang, J. Refik-Rogers, J. Pines, D.J. Wolgemuth, and A. Koff. 2002. Characterization and expression of mammalian cyclin b3, a prepachytene meiotic cyclin. *J. Biol. Chem.* 277:41960–41969. <https://doi.org/10.1074/jbc.M203951200>
- Niemierko, A. 1981. Postimplantation development of CB-induced triploid mouse embryos. *J. Embryol. Exp. Morphol.* 66:81–89.
- Nilsson, J., M. Yekezare, J. Minshall, and J. Pines. 2008. The APC/C maintains the spindle assembly checkpoint by targeting Cdc20 for destruction. *Nat. Cell Biol.* 10:1411–1420. <https://doi.org/10.1038/ncb1799>
- Parry, D.H., and P.H. O'Farrell. 2001. The schedule of destruction of three mitotic cyclins can dictate the timing of events during exit from mitosis. *Curr. Biol.* 11:671–683. [https://doi.org/10.1016/S0960-9822\(01\)00204-4](https://doi.org/10.1016/S0960-9822(01)00204-4)
- Rabut, G., and J. Ellenberg. 2004. Automatic real-time three-dimensional cell tracking by fluorescence microscopy. *J. Microsc.* 216:131–137. <https://doi.org/10.1111/j.0022-2720.2004.01404.x>
- Refik-Rogers, J., K. Manova, and A. Koff. 2006. Misexpression of cyclin B3 leads to aberrant spermatogenesis. *Cell Cycle*. 5:1966–1973. <https://doi.org/10.4161/cc.5.17.3137>
- Rudner, A.D., and A.W. Murray. 2000. Phosphorylation by Cdc28 activates the Cdc20-dependent activity of the anaphase-promoting complex. *J. Cell Biol.* 149:1377–1390. <https://doi.org/10.1083/jcb.149.7.1377>
- Satyanarayana, A., and P. Kaldis. 2009. Mammalian cell-cycle regulation: several Cdks, numerous cyclins and diverse compensatory mechanisms. *Oncogene*. 28:2925–2939. <https://doi.org/10.1038/onc.2009.170>
- Shindo, N., K. Kumada, and T. Hirota. 2012. Separase sensor reveals dual roles for separase coordinating cohesin cleavage and cdk1 inhibition. *Dev. Cell*. 23:112–123. <https://doi.org/10.1016/j.devcel.2012.06.015>
- Sigrist, S., H. Jacobs, R. Stratmann, and C.F. Lehner. 1995. Exit from mitosis is regulated by Drosophila fizzy and the sequential destruction of cyclins A, B and B3. *EMBO J.* 14:4827–4838. <https://doi.org/10.1002/j.1460-2075.1995.tb00164.x>
- Stemmann, O., I.H. Gorr, and D. Boos. 2006. Anaphase topsy-turvy: Cdk1 a securin, separase a CKI. *Cell Cycle*. 5:11–13. <https://doi.org/10.4161/cc.5.1.2296>
- Tarailo-Graovac, M., and N. Chen. 2012. Proper cyclin B3 dosage is important for precision of metaphase-to-anaphase onset timing in *Caenorhabditis elegans*. *G3 (Bethesda)*. 2:865–871. <https://doi.org/10.1534/g3.112.002782>
- Thornton, B.R., and D.P. Toczyski. 2003. Securin and B-cyclin/CDK are the only essential targets of the APC. *Nat. Cell Biol.* 5:1090–1094. <https://doi.org/10.1038/ncb1066>
- Uhlmann, F., F. Lottspeich, and K. Nasmyth. 1999. Sister-chromatid separation at anaphase onset is promoted by cleavage of the cohesin subunit Scc1. *Nature*. 400:37–42. <https://doi.org/10.1038/21831>
- Vázquez-Novelle, M.D., L. Sansregret, A.E. Dick, C.A. Smith, A.D. McAinsh, D. W. Gerlich, and M. Petronczki. 2014. Cdk1 inactivation terminates mitotic checkpoint surveillance and stabilizes kinetochore attachments in anaphase. *Curr. Biol.* 24:638–645. <https://doi.org/10.1016/j.cub.2014.01.034>

- Wu, H., Y. Chen, J. Liang, B. Shi, G. Wu, Y. Zhang, D. Wang, R. Li, X. Yi, H. Zhang, et al. 2005. Hypomethylation-linked activation of PAX2 mediates tamoxifen-stimulated endometrial carcinogenesis. *Nature*. 438: 981-987. <https://doi.org/10.1038/nature04225>
- Yu, H.G., and D. Koshland. 2005. Chromosome morphogenesis: condensin-dependent cohesin removal during meiosis. *Cell*. 123:397-407. <https://doi.org/10.1016/j.cell.2005.09.014>
- Yuan, K., and P.H. O'Farrell. 2015. Cyclin B3 is a mitotic cyclin that promotes the metaphase-anaphase transition. *Curr. Biol.* 25:811-816. <https://doi.org/10.1016/j.cub.2015.01.053>
- Zhang, T., S.T. Qi, L. Huang, X.S. Ma, Y.C. Ouyang, Y. Hou, W. Shen, H. Schatten, and Q.Y. Sun. 2015. Cyclin B3 controls anaphase onset independent of spindle assembly checkpoint in meiotic oocytes. *Cell Cycle*. 14:2648-2654. <https://doi.org/10.1080/15384101.2015.1064567>